Crosslinked chitosan-dextran sulfate nanoparticle for improved topical ocular drug delivery

Wanachat Chaiyasan,[1,2] Sangly P. Srinivas,[4] Waree Tiyaboonchai[1,2,3]

[1]Department of Pharmaceutical Technology, Faculty of Pharmaceutical Sciences, Naresuan University, Phitsanulok, Thailand; [2]The Center of Excellence for Innovation in Chemistry (PERCH-CIC), Commission on High-Education, Ministry of Education, Thailand; [3]The Center of Excellence in Medical Biotechnology, Naresuan University, Phitsanulok, Thailand; [4]School of Optometry, Indiana University, Bloomington, Indiana, United States

Purpose: To examine the benefits of chitosan-dextran sulfate nanoparticles (CDNs) as a topical ocular delivery system with lutein as a model drug.

Methods: CDNs were developed by polyelectrolyte complexation of positively charged chitosan (CS) and negatively charged dextran sulfate (DS). 1-Ethyl-3-(3-dimethylaminopropyl)-carbodiimide (EDC) and polyethylene glycol 400 (PEG400) were used as co-crosslinking and stabilizing agents, respectively. The influence of these on the properties of CDNs, including drug release and mucoadhesiveness, was examined. The chemical stability of lutein in CDNs (LCDNs) was also examined.

Results: Typically, LCDNs showed a spherical shape, possessing a mean size of ~400 nm with a narrow size distribution. The entrapment efficiency of lutein was in the range of 60%–76%. LCDNs possessing a positive surface charge (+46 mV) were found to be mucoadhesive. The release profile of LCDNs followed Higuchi's square root model, suggesting drug release by diffusion from the polymer matrix. Lutein in LCDNs showed increased chemical stability during storage compared to its solution form.

Conclusions: These characteristics of CDNs make them suitable for drug delivery to the ocular surface.

Instillation as drops on the ocular surface is the most common way of administering drugs to the eye. Unfortunately, this topical route of administration produces poor drug bioavailability. This is because of rapid clearance of the instilled drug, along with blink-induced tear drainage. In fact, <1% typically penetrates the cornea and reaches intraocular structures [1]. In addition to entry into systemic circulation via nasal mucosa, a part of the instilled drug reaches systemic circulation by penetration into conjunctival blood vessels [2]. This limitation can be overcome by a nanoparticle-based drug delivery system that can provide sustained release and increased residence time on the ocular surface [3]. The latter can be achieved through the modification of their surface properties. In a previous study, we reported briefly on the potential of chitosan-dextran sulfate nanoparticles (CDNs) as a candidate system for ocular drug delivery [4].

Chitosan (CS) is an ideal polymeric carrier because it is biocompatible, biodegradable, non-toxic, and bioadhesive, and possesses a high positive charge density. Dextran sulfate (DS), on the other hand, has similar properties but is negatively charged. The contrasting charges on CS and DS enable

preparation of CDNs by polyelectrolyte complexation without involving harsh synthesis steps or toxic organic solvents [4,5]. However, in our previous studies, CDNs showed significant aggregation during storage [4]. Thus, in this study, the next generation of CDNs has been developed using PEG400 and EDC as stabilizing and co-crosslinking agents, respectively. The use of PEG400 is common in the formulation of lubricating eye drops [6–8]. It is also known to increase mucoadhesiveness, leading to enhanced drug penetration [3,9–13]. Being a water-soluble carbodiimide, EDC is widely used as a crosslinking reagent [14–17]. Since it can be easily removed with an aqueous wash after crosslinking, the potential for ocular surface irritation is prevented.

Thus, we have further explored the benefits of CDNs as a topical ocular delivery system, with lutein as a model lipophilic drug. In the eye, lutein blocks blue light and is thought to function as an antioxidant. The efficacy of lutein as an antioxidant stems from the fact that it can quench and scavenge light-induced intracellular reactive oxygen species (ROS) [18–20]. Since ROS accumulation in the lens and macular region of the retina leads to pathological consequences, it is believed that the consumption of lutein may reduce the risk of developing major causes of vision loss, including cataracts and/or age-related macular degeneration [21–23]. However, the use of lutein as an antioxidant is limited by its poor water solubility and susceptibility to instability when exposed to

Correspondence to: Waree Tiyaboonchai, Department of Pharmaceutical Technology, Faculty of Pharmaceutical Science, Naresuan University, Phitsanulok 65000, Thailand; Phone: +66-55-961-873; FAX: +66-55-963-731; email: wareet@nu.ac.th

light and heat [24]. Therefore, it is imperative to develop strategies to enhance its chemical stability and penetration into intraocular structures. Nevertheless, nanoparticle-based drug delivery systems offer many advantages, including protection of incorporating substances from chemical degradation and enabling controlled release. Therefore, the main aim of this study was to investigate the effects of PEG400 and EDC on the properties of lutein-loaded CDNs (LCDNs), including the in vitro dissolution and mucoadhesiveness of LCDNs on the ocular surface. Additionally, lutein stability in the formulation was investigated.

METHODS

Materials: Chitosan shrimp (MW 30 kDa with 95% degree of deacetylation) was obtained from Aquapremier Inc. (Bangkok, Thailand). Dextran sulfate (MW 500,000 Da), 1-ethyl-3-(3- dimethylaminopropyl)-carbodiimide hydrochloride and type II mucin from porcine stomach were purchased from Sigma-Aldrich Chemie GmbH (Steinheim, Germany). Polyethylene glycol 400 was purchased from Namsiang Trading Co., Ltd. (Bangkok, Thailand). Lutein (95% lutein extracted from marigold flower extract) was purchased from KEB Biotechnology Co., Ltd. (Beijing, China). All other chemicals and reagents used were of high-performance liquid chromatography (HPLC) and analytical grade. Deionized (DI) water was used in the preparation of solutions and dispersion of nanoparticles.

Preparation of nanoparticles: CDNs were prepared by a polyelectrolyte complexation technique as reported earlier [4]. A CS solution (1.25 ml; 1%, w/v; dissolved in 1.75% acetic acid) was mixed with DI water (total volume: 20 ml). The resulting solution was combined with an aqueous solution of DS (0.75 ml; 1%, w/v) and homogenized at ~8,000 rpm for 15 min. This was then mixed with an aqueous solution of EDC (0.02 ml; 1%, w/v) and PEG400 (0.07 ml) for an additional 30 min.

To prepare the lutein stock solution, lutein was dissolved in Tween-80 solution (1%, v/v; in dimethyl sulfoxide) to a concentration of 1%, w/v. Just before the start of the experiment, the lutein stock solution was further diluted with ethanol to a final concentration of 0.5%, v/v. LCDNs were prepared similarly to CDNs, but by mixing 0.2 mL of lutein (L) aqueous solution with the CS solution before complexation with DS. In this study, we prepared four different formulations with and without PEG400 and/or EDC: LCDN (L + CS + DS), LCDN-P (L+ CS + DS + PEG400), LCDN-E (L + CS + DS + EDC), and LCDN-PE (L + CS + DS + PEG400 + EDC). All procedures were performed in the dark, at room temperature, and produced in triplicate.

Physicochemical characteristics of nanoparticles: The morphology of the nanoparticles was characterized by scanning electron microscopy (SEM; 1455VP, LEO Electron Microscopy Ltd., Cambridge, UK). LCDNs were dropped on studs with carbon tape, sputter-coated with gold, and then observed at a magnification of 10,000X.

The mean particle size and polydispersity index (PI) were measured by dynamic light scattering (DLS) using a ZetaPALS analyzer (Brookhaven Instruments Corporation, New York, NY) with an aliquot diluted in DI water. The particle size of each sample was measured at 25 °C, a detection angle of 90°, and a wavelength of 659 nm in a 10 mm diameter cell. Each data point was an average of 10 runs, and data were subjected to cumulative analysis to obtain an average hydrodynamic diameter [25].

Formulation	MS ± SD (nm)	PI ± SD	ZP ± SD (mV)	Lutein ± SD (µg/ml)	EE ± SD (%)
CDN	296±5	0.28±0.01	52.8±1.2	-	-
LCDN	428±1	0.28±0.01	46.2±0.9	30.36±0.28	60.71±0.55
CDN-P	292±10	0.27±0.02	36.4±1.6	-	-
LCDN-P	451±6	0.29±0.01	38.0±1.8	36.38±1.08	72.76±2.16
CDN-E	296±4	0.24±0.01	33.7±0.5	-	-
LCDN-E	447±6	0.26±0.02	34.1±1.7	36.87±1.27	73.74±2.54
CDN-PE	334±3	0.26±0.01	31.8±0.2	-	-
LCDN-PE	454±7	0.28±0.01	34.4±3.1	38.09±0.65	76.17±1.30

TABLE 1. MEAN PARTICLE SIZE, POLYDISPERSITY INDEX, ZETA-POTENTIAL AND ENTRAPMENT EFFICIENCY OF LUTEIN-LOADED CDNS AND UNLOADED-CDNS.

*MS: mean size; PI: polydispersity index; ZP: zeta potential; EE: entrapment efficiency; SD: standard deviation

The zeta potential (ZP) was determined by phase analysis of light scattering to determine the electrophoretic mobility of charged particles using a ZetaPALS analyzer. Samples were prepared by re-dispersing the CDNs in DI water at 25 °C. The ZP was calculated from the electrophoretic mobility using the Smoluchowski approximation [26]. Each data point was an average of 10 runs.

The entrapment efficiency (EE) of LCDNs was determined as follows. One milliliter of LCDNs was centrifuged at 18,620 ×g for 30 min. The supernatant was discarded and lutein was extracted from the sedimented pellets by sonication with 1 mL of ethanol for 20 s. The lutein in the supernatant, which was obtained after centrifugation at 18,620 ×g for 30 min, was analyzed using a UV-Vis spectrophotometer (446 nm). EE was calculated as [(Amount of lutein extracted) × 100/(Initial amount of lutein)]. Reported EE is based on the mean of three independent trials.

Fourier transform infrared spectroscopy (FTIR): FTIR spectra was obtained using a Spectrum GX series (Perkin-Elmer, MA, USA) equipped with a mirtgs detector and an extkbr beamsplitter. The spectra were obtained in the 4000–700 cm^{-1} range from the KBr disc at 4 cm^{-1} resolution under a dry air purge and reported as an average of 16 scans. The spectrum of the KBr disc was subtracted from each sample spectrum.

In vitro drug release studies: The shake-flask method was employed to assess the release profile of lutein from LCDNs. Since lutein possesses poor aqueous solubility, normal saline solution (NSS, pH 6.5) containing 1% (v/v) Tween-80, was used as a dissolution medium to provide a sink condition. A known amount of LCDNs, consisting of 25 μg/ml of lutein, was mixed into 10 ml of the dissolution medium and shaken (100 rpm) at 34 °C in the dark. At predetermined time intervals of 5, 30, 60, 120, 180, 240, and 360 min, a 1 ml sample was taken and replaced by 1 mL fresh dissolution medium. The samples were then centrifuged at 18,620 ×g for 30 min and the supernatant was assayed for the amount of lutein released using the UV-VIS spectrophotometer (446 nm). All the dissolution experiments were performed in triplicate.

Stability of LCDNs: Four formulations of LCDNs (LCDN, LCDN-P, LCDN-E, and LCDN-PE) were stored in darkness for four weeks at 4 °C and room temperature. A known amount of each formulation containing 70 μg/ml of lutein was mixed in Feldman ophthalmic buffer (10 ml; pH=6)
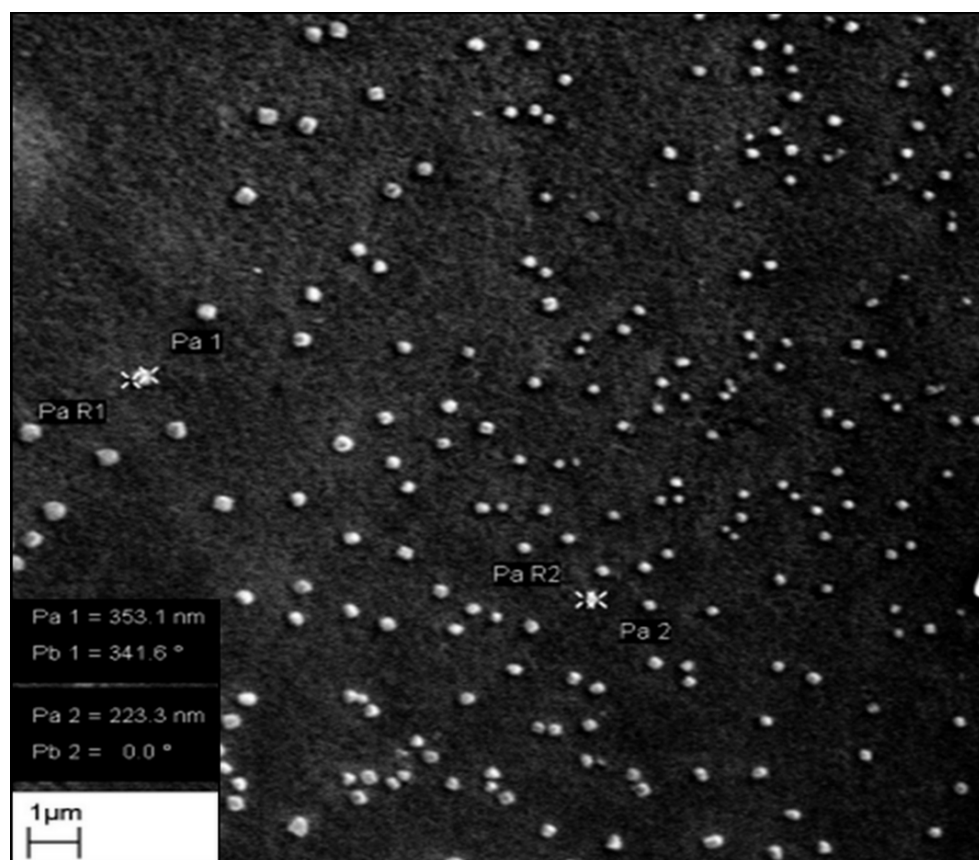

Figure 1. Scanning electron micrograph of lutein-loaded chitosan–dextran sulfate nanoparticles (LCDNs) obtained by formulation with PEG-400 and EDC (LCDN-PE). This was prepared by mixing chitosan (CS): dextran sulfate (DS) ratio of 1:1.67 (by weight), 0.001% w/v 1-ethyl-3-(3-dimethylaminopropyl)-carbodiimide hydrochloride (EDC), and 0.35% v/v polyethylene glycol-400 (PEG-400) with 0.005% v/v lutein aqueous solution. The particles show a spherical shape with uniform particle size distribution. Images for all other formulations showed similar morphology.
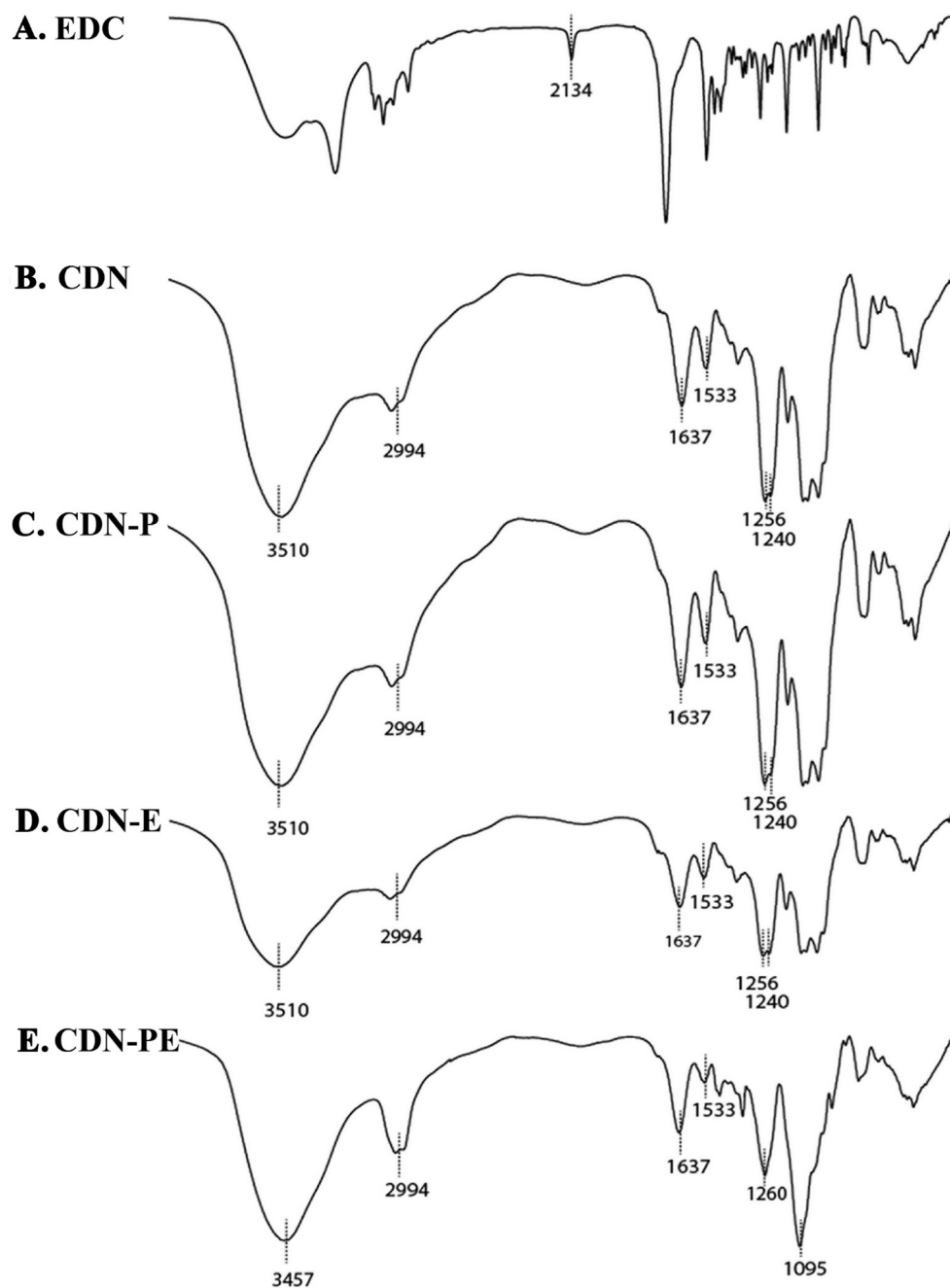
A. EDC

2134

B. CDN

1533
1637
2994
3510
1256
1240

C. CDN-P

1533
1637
2994
3510
1256
1240

D. CDN-E

1533
1637
2994
3510
1256
1240

E. CDN-PE

1533
1637
2994
1260
3457
1095

Figure 2. Characterization of CDN formulations by Fourier transform infrared spectroscopy. FTIR spectra are shown for are EDC powder (**A**), CDN (**B**), CDN-P (**C**), CDN-E (**D**), and CDN-PE (**E**). A KBr disc was used for holding the samples.

and held in an amber glass bottle with headspace filled with nitrogen gas. At predetermined time intervals, particle size and surface charge were monitored by the ZetaPALS analyzer and the lutein content was examined by high-performance liquid chromatography (HPLC) [27].

An HPLC system (Model LD10A, Shimadzu, Kyoto, Japan) equipped with a carotenoid HPLC column (VertiSep™ BIO C30, 4.6×250 mm, 5 µm, Vertical® Thailand) was used. The mobile phase consisted of 2-propanol, dichloromethane,

and methanol (20:10:70). The flow rate was at 1.0 mL/min, and the detection wavelength was 446 nm. All data were processed with the LC Solution® software (Shimadzu, Kyoto, Japan).

In vitro mucoadhesion study: In vitro mucoadhesion of LCDNs was assessed with newly formed mucous membranes. A hydrophilic cellulose nitrate membrane (0.22 µm pore size, 12 mm diameter) was soaked in 0.1% of an aqueous mucin solution for 2 h. Then, 20 µl of LCDNs suspension was
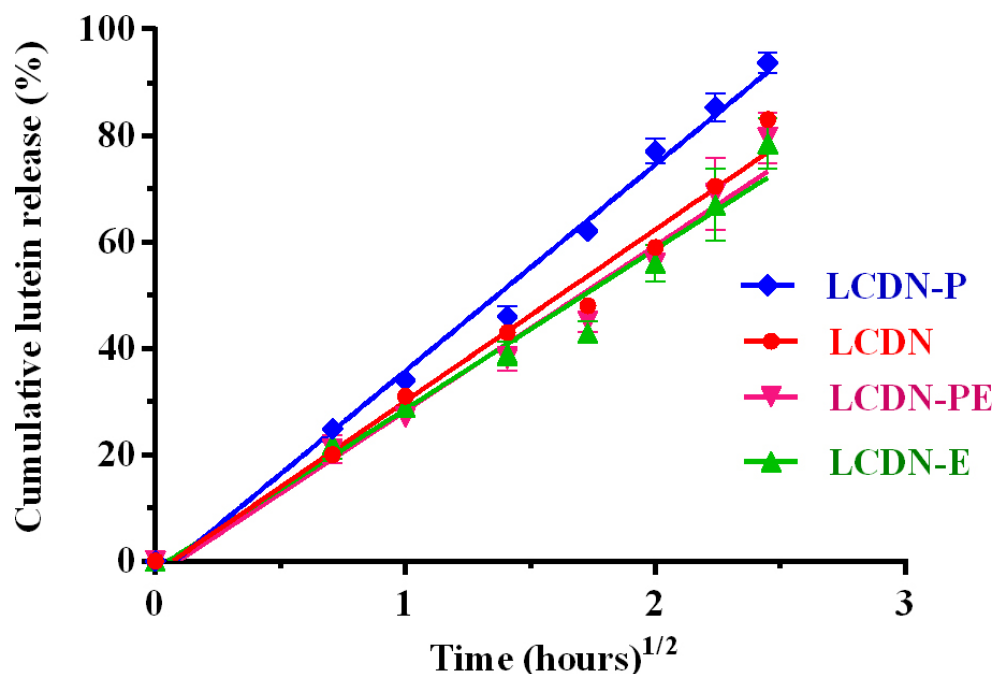
Figure 3. The in vitro dissolution profile of lutein from LCDNs. Normal saline solution (NSS) containing 1% (v/v) Tween-80 were used as dissolution media. All formulations showed an initial burst release (~25%) in the first 30 min, followed by a slow release for 6 h (up to 70%). LCDN-P significantly enhanced drug release rate compared to LCDN, LCDN-E, and LCDN-PE, which demonstrated similar release profiles. (One way ANOVA followed by Tukey's post hoc test, p-value <0.05). Error bars show the standard deviation (n=3).

applied at the center of the membrane. The membrane was then irrigated continuously with NSS at 34 °C for 5 and 60 min at a rate of 10 mL/min. The amount of lutein retained on the mucous membrane was extracted using 1 mL of ethanol, sonication for 20 s, and centrifugation at 18,620 × *g* for 30 min. The supernatant was collected and assayed for lutein using a UV-VIS spectrophotometer (446 nm). The percentage of LCDNs retained on the membrane was calculated as

[(Amount of lutein remaining on the mucous membrane) × 100/(Initial amount lutein instilled)].

Statistical analysis: The results are expressed as mean ± standard deviation (SD). Differences between the groups were compared by one-way ANOVA followed by Tukey's post hoc test. The results were considered to be statistically significant at p<0.05.

TABLE 2. MEAN SIZE, SURFACE CHARGE AND LUTEIN REMAINING OF LCDNS AFTER 4 WEEK STORAGE AT DIFFERENT TEMPERATURES.

Formulations	Temp.	MS ± SD (nm)		ZP ± SD (mV)		Lutein remaining ± SD (%)	
		2 Weeks	4 Weeks	2 Weeks	4 Weeks	2 Weeks	4 Weeks
LCDN	4 °C	P	P	P	P	87.4±3.1	76.9±22.4
	RT	P	P	P	P	44.2±1.9	12.5±2.0
LCDN-P	4 °C	434±10	395±25	39.2±0.9	34.6±0.9	88.4±5.1	87.4±3.5
	RT	423±8	494±25	33.5±2.0	34.9±1.4	46.4±4.2	10.3±0.6
LCDN-E	4 °C	436±10	412±15	37.8±3.5	36.4±1.6	88.2±7.8	86.9±6.6
	RT	438±8	485±35	33.5±2.5	33.7±3.8	53.1±4.1	14.0±1.7
LCDN-PE	4 °C	447±11	417±18	37.9±4.6	35.2±2.1	89.2±14.7	87.1±15.9
	RT	432±12	487±22	35.3±2.6	32.4±1.3	47.4±8.8	11.3±1.2
Lutein solution	4 °C	-	-	-	-	21.3±5.2	15.1±3.6
	RT	-	-	-	-	22.0±5.0	10.3±3.1

*MS: mean size; ZP: zeta potential; P: precipitation; RT: room temperature; Temp: Temperatures; SD: standard deviation

RESULTS

Physicochemical characteristics of nanoparticles: DLS studies of LCDNs showed a mean particle size in the range of 296 to 454 nm with PI <0.3, indicating a narrow size distribution (Table 1). When PEG400 or/and EDC were employed in the preparation of LCDNs, a decrease in zeta potential from +52 mV to +31 mV was observed (Table 1). The EE of lutein into CDNs showed a sharp increase in mean particle size by ~30%, but there was no effect on the zeta potential. The highest EE, up to 76%, was observed in LCDN-PE, followed by LCDN-E and LCDN-P, respectively, whereas a 60% EE was observed in LCDN (Table 1). Observations of nanoparticles via SEM showed a spherical particle with a uniform distribution in all formulations. An example image is shown in Figure 1. The morphological properties were unaffected by the addition of PEG400 or EDC.

FTIR studies: The FTIR spectra of different CDNs (i.e., CDN, CDN-P, CDN-E, and CDN-PE) are shown in Figure 2. All particles showed the same characteristic peaks of FTIR spectra, except CDN-PE. The spectra of CDN, CDN-E, and CDN-P showed patterns similar to those in our previous study, such as spectral shifts in the amine and sulfate regions [4]. This confirms an involvement of electrostatic interactions between cationic CS and anionic DS. Interestingly, the specific effects of PEG400 and EDC were apparent in the spectra of CDN-PE. It showed a broadening of the absorption peak of O-H stretching, as well as a shift to a lower wavenumber (3457 cm^{-1}) and the novel peak of ether linkages (C-O-C) at 1095 cm^{-1}. Figure 2A shows the EDC-dependent

n=C=N vibration peak at 2134 cm^{-1}. This was not detected in CDN-E and CDN-PE (Figure 2D,E).

In vitro drug release: All formulations showed a biphasic drug release profile with an initial burst release (~25%) in the first 30 min, followed by a slow release for 6 h (Figure 3). The mechanism of the slow release phase was analyzed by fitting with three kinetic models: zero-order, first-order, and the Higuchi square root model. Based on the correlation coefficient (R^2), the release profiles of all LCDNs could be best fit to the Higuchi square root model (R^2=0.98–0.99). This indicates that lutein released from CDNs in the second phase occurs by a diffusion-controlled mechanism from the polymer matrix. The use of EDC and PEG400 affected lutein release kinetics very slightly. LCDN-P showed the highest drug release rate compared to those of LCDN, LCDN-E, and LCDN-PE, which demonstrated similar release profiles.

Stability of LCDNs: After storage at 4 °C and room temperature for four weeks, the formulations LCDN-E, LCDN-P, and LCDN-PE showed similar mean particle sizes and surface charges (Table 2) without any evidence of aggregation or precipitation. However, the LCDN formulation showed precipitation. Furthermore, at room temperature, the lutein solution and lutein in LCDNs were found to degrade rapidly; only 15% was detected after four weeks of storage (Table 2). Conversely, after four weeks of storage at 4 °C, only 13% of lutein in LCDNs degraded. Nevertheless, lutein in the solution was degraded by 85% at 4 °C.

In vitro mucoadhesive study: The mucoadhesive properties of nanoparticles were examined in vitro using a membrane
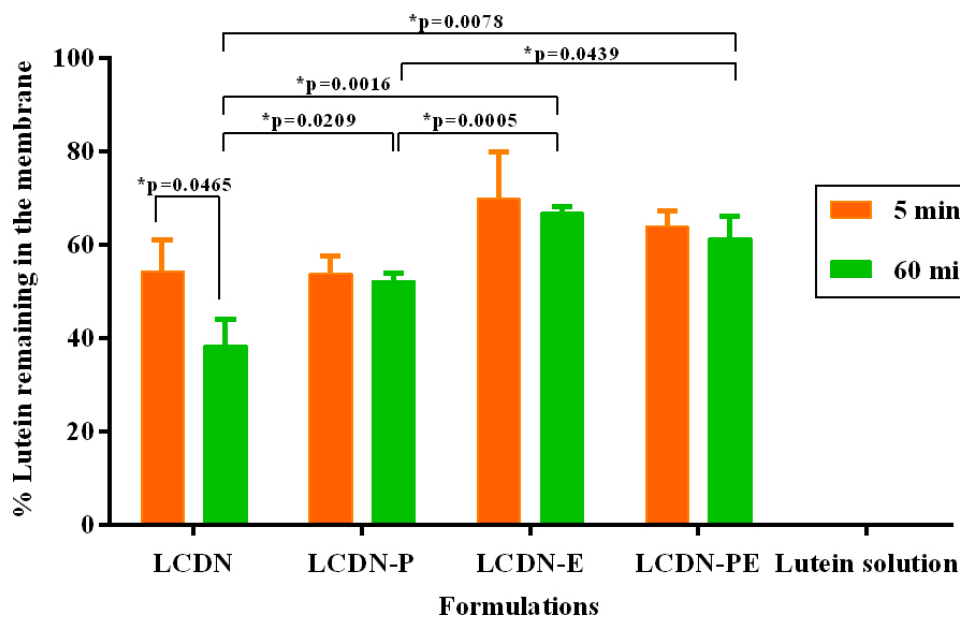

Figure 4. The percentage of lutein remaining on the mucous membrane after a steady flow of normal saline solution (NSS) at 5 min (orange bar) and 60 min (green bar; *One way ANOVA followed by Tukey's post hoc test, p-value <0.05). For all formulations, lutein retained on the membrane was >50% after 5 min and >40% after 60 min under fluid flow, respectively. Error bars show the standard deviation (n=3).

coated with mucin to simulate the ocular surface. As shown in Figure 4, instillation of lutein solution onto the mucous membrane resulted in a significant loss of lutein within 5 min of fluid flow. With instillation of LCDNs, however, more than 40% of lutein was retained even after 60 min of fluid flow. This shows a substantial increase in mucoadhesiveness with LCDNs. The addition of PEG400 and EDC into LCDNs further increased mucoadhesiveness. After 5 min of fluid flow, LCDN-E showed the greatest retention on the mucous membrane, followed by LCDN-PE, LCDN-P, and LCDN, respectively. There were no significant differences observed in the three formulations—LCDN-E, LCDN-P and LCDN-PE—when compared between 5 min and 60 min, while LCDN showed that the remaining lutein significantly decreased on the mucous membrane after 60 min.

DISCUSSION

As shown previously, CDNs can be produced by the polyelectrolyte complexation technique [4]. However, such particles obtained by mere polyelectrolyte complexation show significant aggregation. Thus, PEG400 was added as a stabilizer to prevent aggregation of CDNs, while EDC was added as a co-crosslinker to enhance the density of the polymer matrix. The specific effects of PEG400 and EDC are evident in the FTIR spectra of CDN-PE. The broadening of the absorption peak of O-H stretching suggests the formation of a large number of inter- and intra-molecular hydrogen bonds between hydroxyl groups of CS, DS, and PEG400 [28]. The novel peak of ether linkage at 1095 cm^{-1} indicates crosslinking within the polymer matrix secondary to intermediate-carbodiimide for primary alcoholic groups (R-C-OH) of CS, DS, and PEG400 [29]. However, the ether linkage peak could not be detected in the FTIR spectra of CDN-E. This may be due to a smaller number of ether linkages, but this could not be confirmed. Moreover, the carbodiimide peak (n=C=N) of EDC could not be detected in CDN-E and CDN-PE. This indicates that EDC was washed off and not incorporated into CDN-E and CDN-PE [29]. Thus, EDC was an intermediate cross-linker in CDN-E and CDN-PE.
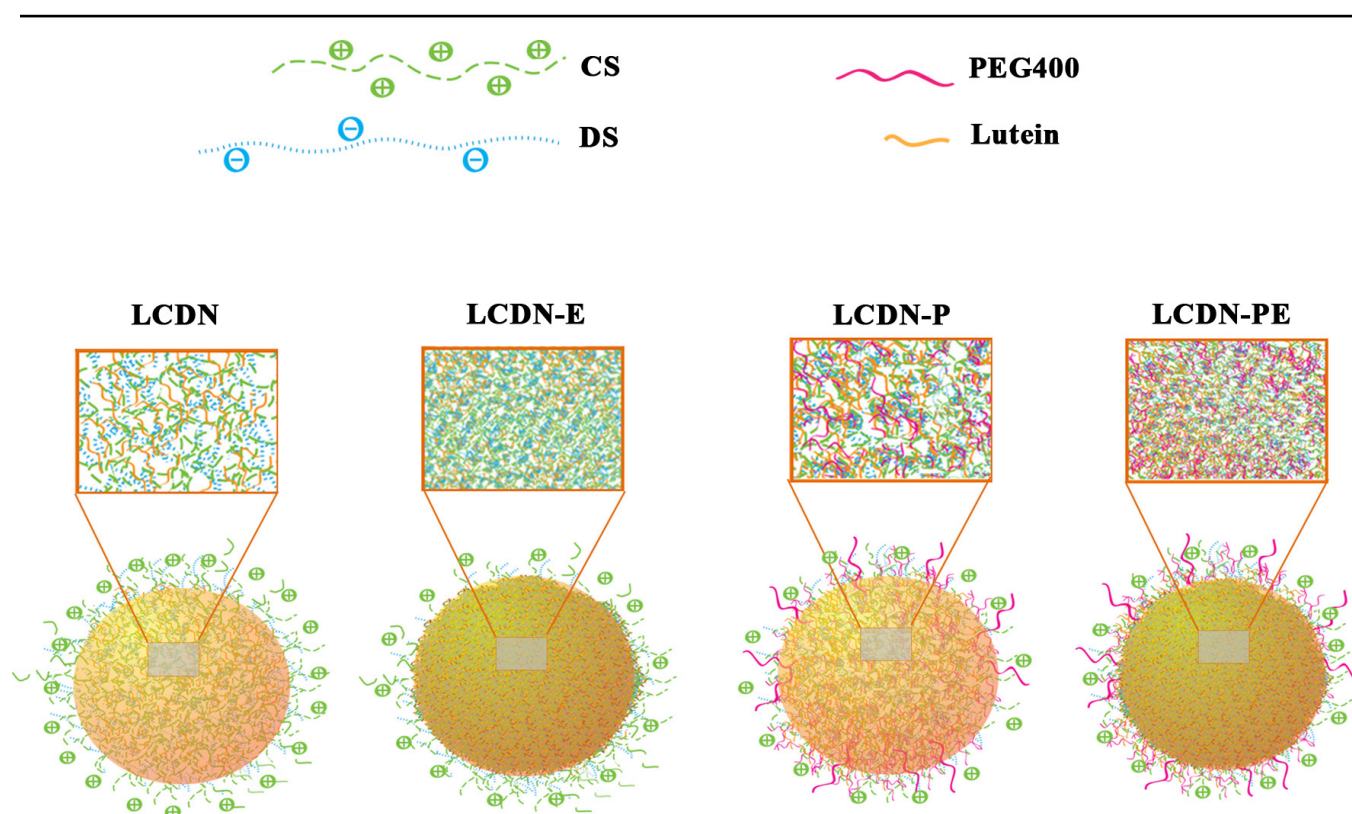

Figure 5. A proposed structural model for LCDNs. CS is indicated by green lines. DS is shown by blue lines. Lutein is shown by orange lines. PEG-400 is in pink lines. LCDN contains CS, DS, and lutein. LCDN-P consists of CS, DS, lutein, and PEG400. LCDN-E is composed of CS, DS, and lutein. (EDC is not shown, as it is removed upon washing of the nanoparticles.) LCDN-PE is composed of CS, DS, PEG400, and lutein. Lutein is incorporated into the polymer matrix and entrapped in CDNs via hydrophobic interactions and/or hydrogen bonding. PEG400 is located around the particle surface and is postulated to interact with lutein.

LCDNs are intended for the ocular surface, and so their size and surface charges are important. In general, the particle size should not exceed 10 μm; larger-sized particles can scratch the highly innervated ocular surface during blinking and lead to irritation and patient discomfort [30,31]. All developed LCDNs showed a mean size <400 nm with narrow size distribution and hence are suitable for topical administration to the eye. The addition of EDC and/or PEG400 did not significantly affect the particle size, but the decrease in zeta potential was observed. This could be due to the formation of hydrogen bonding between PEG400 and free amine groups of CS [32,33]. EDC, as an intermediate crosslinker, could induce polymer chains to come closer to each other by formation of ether linkages between the primary alcoholic groups [29]. This could increase the probability for free amine groups on the CS to form inter- and intramolecular bonding.

The entrapment efficiency of lutein was also affected by the addition of PEG400 and EDC. LCDNs prepared with EDC and/or PEG400 showed high drug EE of ~76% compared to LCDN, 60%, indicating that the EDC and PEG400 could enhance drug incorporation efficiency. This could be due to the increased density of the polymer matrix because of EDC that might increase the diffusional resistance of drug molecules from the polymer matrix to the medium, while PEG400 was believed to interact with hydroxyl group of unentrapped lutein via hydrogen bonding and then inserted inside the polymer matrix or located on the particle surface.

Interestingly, the release profile of LCDNs was found to be dependent on the position of lutein with nanoparticles that could be attributed to two potential mechanisms. The first, initial fast release or burst release phase could be attributed to the release of lutein bound to the particle surface [34,35]. The second, slower release phase might be attributed to pore formation of the polymer matrix by a diffusion-controlled mechanism. As expected, LCDN-P, the formulation with PEG400, significantly enhanced the release rate of the drug (p<0.05) compared to LCDN, LCDN-E, and LCDN-PE, which demonstrated similar release profiles. This finding could be postulated by two mechanisms. First, lutein could be bound to PEG400 localized at the particle surface. Second, water-soluble PEG400 might be incorporated into the polymer matrix, and it could be easily leached out into the dissolution medium, leading to pore formation in the polymer matrix. Similarly, several reports suggest that PEG could accelerate and modulate the release of several compounds, such as ovalbumin, immunoglobulin, and dextran [3,36,37]. The release profiles of LCDN, LCDN-E, and LCDN-PE showed similar release rates in 6 h. However, after 30 min, the LCDN-PE and LCDN-E showed a lutein release rate slightly lower than

that of LCDN, which conforms to statements above that EDC might act as an intermediary in the cross-linking reaction leading to the dense polymer matrix.

The physical stability of chitosan nanoparticles is a top concern due to their instability in the liquid form [38,39]. In this study, all nanoparticles showed good stability of the colloidal suspension without evidence of aggregation or precipitation at both storage temperatures, except LCDN. Considering that all nanoparticles possessed a high zeta potential, the observation suggested that electrostatic repulsion forces were not enough to prevent particle aggregation. Interestingly, the addition of EDC and PEG400 could enhance the physical stability of the colloidal suspension. PEG400 was believed to prevent particle aggregation via a steric hindrance mechanism by acting as protective colloids [40,41], whereas EDC could act as a hardening agent by creating a high cross-link density, leading to a reduction in the degree of swelling, thereby preventing particle aggregation [42].

Meanwhile, the chemical stability of lutein in nanoparticles is also an important issue. Although the long polyene chain of lutein is advantageous for light absorption, it is notorious for its instability and could be easily degraded by oxidation, especially during high-temperature storage [24,43]. As expected, the results support the hypothesis that the incorporation of lutein into CDNs should protect the lutein from decomposition. Also conforming to expectation, LCDN suspension showed excellent lutein protection, more than the lutein solution form, especially the formulation with EDC and/or PEG400 (Table 2). This improvement of lutein stability was probably attributed to the high crosslinking density of the polymeric matrix that reduced the swelling degree in the polymeric matrix, making it difficult for the aqueous medium to diffuse into nanoparticles. These results indicate that CDNs could improve lutein stability.

Interestingly, LCDNs could not only improve the entrapment efficacy and stability of lutein but also enhance the lutein accumulation on the ocular surface by mucoadhesive performance of nanoparticles. All LCDNs showed good adhesion to the mucous membrane compared to the lutein solution. The lutein solution was removed rapidly by fluid flow, indicating that lutein could not adhere to the mucous membrane by itself. The possibility of LCDN adhesion can be attributed to electrostatic interactions between a positively charged CS and a negatively charged mucin [4]. Additionally, the hydroxyl and amino groups of CS may also interact with mucin via hydrogen bonds [3,4]. Moreover, the mucoadhesive performance of LCDNs could be enhanced by the addition of PEG400 and/or EDC. PEG400 is believed to act as a mucoadhesion promoter by the interpenetration of polymer

chains into the mucus layer [3,44]. EDC could facilitate a high crosslink density, thus reducing the degree of swelling and contributing to the difficulty of removal from the mucous in the presence of high humidity [45]. In contrast, a less cross-linked polymer matrix, like LCDN, could be more easily removed from the mucous membrane because of its hydrophilic properties that increase the degree of swelling, leading to a slippery tractionless surface [46]. Based on these results, it can be concluded that LCDNs and the mucosal surface are closely bound by electrostatic attraction and hydrogen bonding. This could be useful to prolonging the contact time of a drug delivery system in the mucosa and improve the treatment efficacy of lutein or/and other drugs.

Based on our data, a structure of LCDNs is proposed in Figure 5. LCDNs are mainly composed of a CS-DS matrix. PEG400 could be located both in the CS-DS polymer matrix and coated on the particle surface through ether linkages or hydrogen bonds. Lutein is incorporated into the polymer matrix, while some is adsorbed on the particle surface. EDC increases the density of the polymer matrix and is easily removed from the particles by irrigation.

Conclusions: LCDNs were successfully developed to improve potential drug delivery to the ocular surface. The addition of PEG400 and EDC could improve physical stability, enhance ocular surface retention time, and provide sustained release characteristics. The chemical stability of lutein incorporated into CDNs was significantly improved compared to lutein in solution. In optimal conditions, the developed LCDNs showed a mean particle size of <500 nm, which is unlikely to cause any abrasive injury to the ocular surface. Overall, the mucoadhesive LCDNs exhibit characteristics suitable for topical ocular drug delivery, including (1) ease of manufacturing and mild conditions during preparation, (2) avoidance of organic solvents, (3) controlled drug release, (4) high entrapment efficiency, and (5) mucoadhesiveness.

APPENDIX 1

To access the data, click or select the words "Appendix 1." Regression linear equation and correlation coefficient (R^2) of three different drug release kinetic models.

ACKNOWLEDGMENTS

REFERENCES

1. Wagh VD, Inamdar B, Samanta MK. Polymers used in ocular dosage form and drug delivery systems. Asian J Pharm 2008; 2:12-7. .

2. Gaudana R, Ananthula HK, Parenky A, Mitra AK. Ocular drug delivery. AAPS J 2010; 12:348-60. [PMID: 20437123].

3. Bin Choy Y, Park J-H, Prausnitz MR. Mucoadhesive microparticles engineered for ophthalmic drug delivery. J Phys Chem Solids 2008; 69:1533-6. [PMID: 20657721].

4. Chaiyasan W, Srinivas SP, Tiyaboonchai W. Mucoadhesive chitosan-dextran sulfate nanoparticles for sustained drug delivery to the ocular surface. J Ocul Pharmacol Ther 2013; 29:200-7. [PMID: 23356788].

5. Zhang Z, Nix CA, Ercan UK, Gerstenhaber JA, Joshi SG, Zhong Y. Calcium binding-mediated sustained release of minocycline from hydrophilic multilayer coatings targeting infection and inflammation. PLoS ONE 2014; 9:e84360- [PMID: 24409292].

6. Davitt WF, Bloomenstein M, Christensen M, Martin AE. Efficacy in patients with dry eye after treatment with a new lubricant eye drop formulation. J Ocul Pharmacol Ther 2010; 26:347-53. [PMID: 20653478].

7. Foulks GN. Clinical evaluation of the efficacy of PEG/PG lubricant eye drops with gelling agent (HP-Guar) for the relief of the signs and symptoms of dry eye disease: a review. Drugs Today (Barc) 2007; 43:887-96. [PMID: 18174974].

8. Springs C. Novel ocular lubricant containing an intelligent delivery system: details of its mechanism of action. Dev Ophthalmol 2010; 45:139-47. [PMID: 20502034].

9. Fresta M, Panico AM, Bucolo C, Giannavola C, Puglisi G. Characterization and in-vivo ocular absorption of liposome-encapsulated acyclovir. J Pharmacol Pharmacother. 1999; 51:565-76. [PMID: 10411216].

10. Giannavola C, Bucolo C, Maltese A, Paolino D, Vandelli MA, Puglisi G, Lee VH, Fresta M. Influence of preparation conditions on acyclovir-loaded poly-d,l–lactic acid nanospheres and effect of PEG coating on ocular drug bioavailability. Pharm Res 2003; 20:584-90. [PMID: 12739765].

11. Lai SK, O'Hanlon DE, Harrold S, Man ST, Wang Y-Y, Cone R, Hanes J. Rapid transport of large polymeric nanoparticles in fresh undiluted human mucus. Proc Natl Acad Sci USA 2007; 104:1482-7. [PMID: 17244708].

12. Wang Y-Y, Lai SK, So C, Schneider C, Cone R, Hanes J. Mucoadhesive nanoparticles may disrupt the protective human mucus barrier by altering its microstructure. PLoS ONE 2011; 6:e21547-[PMID: 21738703].

13. Wang Y-Y, Lai SK, Suk JS, Pace A, Cone R, Hanes J. Addressing the PEG mucoadhesivity paradox to engineer nanoparticles that "slip" through the human mucus barrier.

Angew Chem Int Ed Engl 2008; 47:9726-9. [PMID: 18979480].

14. Bennet D, Marimuthu M, Kim S, An J. Dual drug-loaded nanoparticles on self-integrated scaffold for controlled delivery. Int J Nanomedicine 2012; 7:3399-419. [PMID: 22888222].

15. Duan X, Sheardown H. Dendrimer crosslinked collagen as a corneal tissue engineering scaffold: Mechanical properties and corneal epithelial cell interactions. Biomaterials 2006; 27:4608-17. [PMID: 16713624].

16. Lai JY, Ma DH, Cheng HY, Sun CC, Huang SJ, Li YT, Hsiue GH. Ocular biocompatibility of carbodiimide cross-linked hyaluronic acid hydrogels for cell sheet delivery carriers. J Biomater Sci Polym Ed 2010; 21:359-76. [PMID: 20178691].

17. Wu Y, Yao J, Zhou J, Dahmani FZ. Enhanced and sustained topical ocular delivery of cyclosporine A in thermosensitive hyaluronic acid-based in situ forming microgels. Int J Nanomedicine 2013; 8:3587-601. [PMID: 24092975].

18. Roberts JE. Ultraviolet radiation as a risk factor for cataract and macular degeneration. Eye Contact Lens 2011; 37:246-9. [PMID: 21617534].

19. Chitchumroonchokchai C, Schwartz SJ, Failla ML. Assessment of lutein bioavailability from meals and a supplement using simulated digestion and caco-2 human intestinal cells. J Nutr 2004; 134:2280-6. [PMID: 15333717].

20. He RR, Tsoi B, Lan F, Yao N, Yao XS, Kurihara H. Antioxidant properties of lutein contribute to the protection against lipopolysaccharide-induced uveitis in mice. Chin Med 2011; 6:38-[PMID: 22040935].

21. Moeller SM, Voland R, Tinker L, Blodi BA, Klein ML, Gehrs KM, Johnson EJ, Snodderly DM, Wallace RB, Chappell RJ, Parekh N, Ritenbaugh C, Mares JA. the CSG. Associations between age-related nuclear cataract and lutein and zeaxanthin in the diet and serum in the Carotenoids in Age-Related Eye Disease Study (CAREDS), an ancillary study of the Women's Health Initiative. Arch Ophthalmol 2008; 126:354-64. [PMID: 18332316].

22. Karppi J, Laukkanen JA, Kurl S. Plasma lutein and zeaxanthin and the risk of age-related nuclear cataract among the elderly Finnish population. Br J Nutr 2012; 108:148-54. [PMID: 22005336].

23. Liu XH, Yu RB, Liu R, Hao ZX, Han CC, Zhu ZH, Ma L. Association between lutein and zeaxanthin status and the risk of cataract: a meta-analysis. Nutrients. 2014; 6:452-65. [PMID: 24451312].

24. Shi XM, Chen F. Stability of lutein under various storage conditions. Nahrung 1997; 41:38-41. .

25. Koppel DE. Analysis of macromolecular polydispersity in intensity correlation spectroscopy: The method of cumulants. J Chem Phys 1972; 57:4814-20. .

26. McNeil-Watson F, Tscharnuter W, Miller J. A new instrument for the measurement of very small electrophoretic mobilities using phase analysis light scattering (PALS). Colloids Surf A Physicochem Eng Asp 1998; 140:53-7. .

27. Niamprem P, Rujivipat S, Tiyaboonchai W. Development and characterization of lutein-loaded SNEDDS for enhanced absorption in Caco-2 cells. Pharm Dev Technol 2014; 19:735-42. [PMID: 23985012].

28. Fan M, Dai D, Huang B. Fourier transform infrared spectroscopy for natural fibres. In: Salih SM, editor. Fourier Transform - Materials Analysis: InTech, Rijieka, 2012. p. 45–68.

29. Banegas RS, Zornio CF. Borges AdMG, Porto LC, Soldi V. Preparation, characterization and properties of films obtained from cross-linked guar gum. Polímeros. 2013; 23:182-8. .

30. Gonzalez-Mira E, Egea MA, Garcia ML, Souto EB. Design and ocular tolerance of flurbiprofen loaded ultrasound-engineered NLC. Colloids Surf B Biointerfaces 2010; 81:412-21. [PMID: 20719479].

31. Zimmer A, Kreuter J. Microspheres and nanoparticles used in ocular delivery systems. Adv Drug Deliv Rev 1995; 16:61-73. .

32. Buranachai T, Praphairaksit N, Muangsin N. Chitosan/polyethylene glycol beads crosslinked with tripolyphosphate and glutaraldehyde for gastrointestinal drug delivery. AAPS PharmSciTech 2010; 11:1128-37. [PMID: 20652459].

33. Malhotra M, Lane C, Tomaro-Duchesneau C, Saha S, Prakash S. A novel method for synthesizing PEGylated chitosan nanoparticles: strategy, preparation, and in vitro analysis. Int J Nanomedicine 2011; 6:485-94. [PMID: 21562608].

34. José LA. Key Aspects in Nanotechnology and Drug Delivery. Nanotechnology and Drug Delivery, Volume One: CRC Press; 2014. p. 1–27.

35. Makadia HK, Siegel SJ. Poly lactic-co-glycolic acid (PLGA) as biodegradable controlled drug delivery carrier. Polymers. 2011; 3:1377-97. [PMID: 22577513].

36. Huang CL, Steele TWJ, Widjaja E, Boey FYC, Venkatraman SS, Loo JSC. The influence of additives in modulating drug delivery and degradation of PLGA thin films. NPG Asia Mater. 2013; 5:e54-.

37. Wang F, Lee T, Wang C-H. PEG modulated release of etanidazole from implantable PLGA/PDLA discs. Biomaterials 2002; 23:3555-66. [PMID: 12109679].

38. Jonassen H, Kjøniksen A-L, Hiorth M. Stability of Chitosan Nanoparticles Cross-Linked with Tripolyphosphate. Biomacromolecules 2012; 13:3747-56. [PMID: 23046433].

39. Honary S, Ghajar K, Khazaeli P, Salchian P. Preparation, Characterization and Antibacterial Properties of Silver-Chitosan Nanocomposites Using Different Molecular Weight Grades of Chitosan. Trop J Pharm Res 2011; 10:69-.

40. Fang C, Bhattarai N, Sun C, Zhang M. Functionalized nanoparticles with long-term stability in biological media. Small 2009; 5:1637-41. [PMID: 19334014].

41. Luangtana-Anan M, Limmatvapirat S, Nunthanid J, Chalongsuk R, Yamamoto K. Polyethylene Glycol on Stability of Chitosan Microparticulate Carrier for Protein. AAPS PharmSciTech 2010; 11:1376-82. [PMID: 20821174].

42. Liu Y, Tourbin M, Lachaize S, Guiraud P. Silica Nanoparticle Separation from Water by Aggregation with AlCl3. Ind Eng Chem Res 2012; 51:1853-63. .

43. Subagio A, Wakaki H, Morita N. Stability of Lutein and Its Myristate Esters. Biosci Biotechnol Biochem 1999; 63:1784-6. [PMID: 26300170].

44. He L-h, Xue R, Yang D-b, Liu Y, Song R. Effects of blending chitosan with peg on surface morphology, crystallization and thermal properties. Chin J Polym Sci. 2009; 27:501-10. .

45. McCarron PA, Woolfson AD, Donnelly RF, Andrews GP, Zawislak A, Price JH. Influence of plasticizer type and storage conditions on properties of poly(methyl vinyl ether-co-maleic anhydride) bioadhesive films. J Appl Polym Sci 2004; 91:1576-89. .

46. Shaikh R, Raj Singh TR, Garland MJ, Woolfson AD, Donnelly RF. Mucoadhesive drug delivery systems. J Pharm Bioallied Sci. 2011; 3:89-100. [PMID: 21430958].